# To Express Required CT-Scan Resolution for Porosity and Saturation Calculations in Terms of Average Grain Sizes

**Ahmed Zoeir*[1] and Jafar Qajar[2]**

[1] Faculty of Petroleum and Natural Gas Engineering, Sahand University of Technology, Tabriz, Iran

[2] School of Chemical and Petroleum Engineering, Shiraz University, Shiraz, Iran

## ABSTRACT

Despite advancements in specifying 3D internal microstructure of reservoir rocks, identifying some sensitive phenomenons are still problematic particularly due to image resolution limitation. Discretization study on such CT-scan data always has encountered with such conflicts that the original data do not fully describe the real porous media. As an alternative attractive approach, one can reconstruct porous media to generate pore space representations. The reconstructed structures are then used for simulations using some sort of discretization. In this paper, It is examined the effect of discretization on porosity and saturation calculations in porous media models. Some 3D Boolean models of random overlapping spheres of fixed and variable diameters in three dimensions are used. The generated models are then discretized over 3D grids with different number of voxels. The porosity can be calculated and saturation of the discretized models are then compared with the analytical solutions. The results show that when meshgrid sizes are 8% of smallest grains, porosity is calculated with 95% precision. In addition to that, meshgrid sizes of 5% and

3% of average grain diameter are adequate to calculate non-wetting and wetting phase saturations with at least 95% precision. This helps in choosing the optimum voxel size required in imaging for efficiently use of available computational facility.

**Keywords:** Boolean Model, Discretization, Micro-CT, Mesh-Grid, Model Porous Media, Porosity, Saturation

## INTRODUCTION

The characterization of the microstructure of natural and synthetic porous materials has been of great importance for scientists and engineers over a wide range of disciplines and hence, it has been the subject of numerous studies in various fields. In petroleum engineering, for example, an understanding of the interactions among rock microstructure, mineralogy, and fluids in pore space is crucial to us for better interpretation and prediction of reservoir rock properties and flow processes in underground formations. Development in structural study of porous materials has a long history. Over the past two decades, direct measurements of 3D structures at resolutions down to a few microns using X-ray micro-

**\*Corresponding author**

Ahmed Zoeir

Email: ah_zoeir@sut.ac.ir

Tel: +98 938 4508088

Fax: +98 71 36133753

To Express Required CT-Scan Resolution for Porosity and Saturation Calculations ...

**Journal of Petroleum Science and Technology**

computed tomography (micro- CT) is being used increasingly. CT is considered as a non-destructive imaging technique that uses X–ray technology (XRT) and mathematical reconstruction algorithm to view cross sectional slices of internal structure of rock samples. CT- scan generates slices through the object for different positions during stepwise rotation whereby either the source and detector or the object is moved. From sets of these projections, cross sectional images and then 3D images are reconstructed by applying Fourier transform algorithm. Although the micro-CT technique has evolutionised, the amount of information that we can obtain from a rock sample and several challenges behind the implementation of the method for characterizing the rock microstructure which still exist, limit the usability of the acquired data. In particular, a major limitation of the imaging techniques is finite resolution of the images. First, the finite image resolution makes ambiguity in identifying different materials/phases within the sample. Second, the high-resolution imaging gives rise to very large datasets and hence requires intensive computations, large computer memory, and considerable processing, time, as stated in 2006 [1]. Third, the higher the resolution the smaller the sample and the smaller the sample the fewer the structural properties can be captured in a representative way as declared by, Vogel, Weller, and Schluter in 2010 [2]. This leads to the challenge of detecting the microstructure of the material at finer resolution and then to connect it to the macro-scale where continuum mechanics applies, Liu and Regenauer in 2011 [3]. Due to such difficulties, flow simulations in complex sedimentary rocks based on images are problematic and it is of great interest to use alternative methods to the

direct imaging or to propose the appropriate use of the imaging techniques that can optimize computational resources usage.

As an alternative to direct visualization and characterization, numerical simulations based on simplified representations (models) of rock microstructure have long been employed to obtain an understanding of static and dynamic behavior of rocks at the pore scale, as studied by Adler in 1992 [4], and Sahimi in 2011 [5].

In this regard, a large number of models have been developed to simulate the structure of porous materials. Among them, the Boolean model of randomly distributed grains has successfully employed to represent irregular spatial structures, by Bilodeau, Meyer, and Schmitt in 2007 [6], Torquato in 2005 [7] including reservoir rocks in particular, Arns, Knackstedt, and Mecke in 2009 [8]. Either in the case of micro-CT images or artificial image models of porous media, spatial discretization is required to compute physical properties or to solve differential equations that govern fluid flow. The rock microstructure obtained by digital images has been already naturally discretized as voxels. The artificial image models have also be discretized into a mesh-grid domain. In general, using smaller voxel size in image-based calculations as well as smaller grid- block size in simulation permits more detailed description of porous media. In spite of this, using small voxels/mesh-grids leads to large numbers of voxels/mesh-grids in a fixed size domain and hence large requirements of computational resources. In this regard, it is of great interest to determine the optimum voxel size to which structural details can be sufficiently resolved. In practice, a certain resolution is enough to calculate different reservoir rock properties like

porosity, contact area, and wetting and non-wetting phase saturation. On the other hand, an optimum mesh-grid size in simulation leads to properly use the computational resources. A number of studies have addressed the discretization effects and the associated errors for estimation of the properties of materials. Latief, Irayani, and Fauzi in 2012 [9] used a Skyscan 1173 μ-CT scanner at the Basic Science Advanced Laboratory of the Bandung Institute of Technology to produce images of a sandstone sample at three voxel sizes of 30, 15, and 7.5 μm. They calculated a number of macro- and micro-scale properties including porosity, permeability, and specific surface area to examine the effect of scanning resolution on the physical properties. They showed that the voxel size has a direct influence on the calculated properties. In particular, porosity and tortuosity increase with an increase in voxel size whereas specific surface area and permeability decreases. Ferréol and Rothman in 1995 [10] studied the effect of grid resolution on image-based calculation of permeability using the lattice-Boltzmann method and qualitatively concluded that finer space discretization leads to more accurate estimation of porous media properties. In another work, Pan, Hilpert, and Miller in 2001 [11] studied the discretization effects of permeability calculation during simulation of single phase flow in simulated sphere packing with varying porosity and pore-size distribution. They applied several different sphere pack models that vary in sphere-size distribution to study primitive media properties. They used pore-network calibration onto the size distribution of pore bodies and throats. They also varied voxel sizes to reach discretization independent properties, but their study on discretization effects was only limited to

permeability. Arns et al in 2001 [12] considered major sources of errors, namely finite size effects, discretization errors, and statistical fluctuations in calculation of transport properties of rocks from digitized images. They showed that using different voxel sizes led to different conductivity values. They argued that the discretization errors are due to a number of factors including inaccurate description of curved grain boundaries and closing of narrow pores. They finally concluded that considering discretization errors may lead to scale out the potential error due to channels not being resolved and hence an accurate continuum value for transport properties was obtained. Silin and Patzek in 2009 [13] considered sandstone images as discretized porous media and predicted fluid flow properties using some spherical models for voxels of 5 and 10 percent of grains diameter. They showed good agreements between computed parameters and direct experimental measurements.

The aim of this study is to investigate the effects of discretization on porosity and saturation calculations in order to address a proper voxel/mesh-grid size for practice.

The paper is organized as follows: First, It will be generated some 3D Boolean models of random overlapping spheres of fixed and variable diameters in three dimensions. Then the generated model is discretized over a 3D grid of different number of voxels. After that, It is compared the calculated porosity and saturation of the discretized model with analytical solutions and evaluate the associated errors. Finally, It is applied the proposed procedure for the micro-CT images of two natural sedimentary core samples. The novelty of this study is that we focused on saturation calculation of wetting and non- wetting phases, say water and

To Express Required CT-Scan Resolution for Porosity and Saturation Calculations ...

**Journal of Petroleum Science and Technology**

oil, and expressed calculated adequate resolution in terms of average grain sizes. Knowing oil and water distributions in each section and every pore channel is vital for calculation of capillary pressure curves and also relative permeability curves. Since any preventable error in calculation of saturation distributions that comes from the selection of inadequate resolution will impact on the calculation of relative permeability and capillary pressure curves.

## EXPERIMENTAL PROCEDURES
### The Boolean Model

We used some 3D Boolean models of random overlapping spheres as porous medium prototypes. The Boolean model is a random closed set, a topic belong in the realm of stochastic geometry which deals with mathematical models for random geometric structure, (Schneider and Weil in 2008) [14]. In essence, the Boolean model is constructed by a collection of points, called germs, distributed according to a Poisson point process of intensity λ and a system of objects, called grains, with the specified shape, size, and orientation, Bilodeau, Meyer, and Schmitt in 2005 [15]. The Poisson intensity indicates the mean number of objects per unit volume. The Boolean model includes two types of randomness, i.e., a spatial Poisson distribution of germs characterized by an intensity value, and randomness of the grains specified by the probability distribution of the grains, as Sobczyk, and Kirkner declared in 2012 [16]. In addition, in the Boolean model of overlapping spheres, the grains are spheres with a random radius, and the sphere centers are located on points of a Poisson point process of intensity λ, (Molohanov in 1990) [17]. In this case, the probability distribution of the grains is the distribution of their radius. The density of sphere centers is related to the sphere volume fraction.

## Computational Methods

In this paper, It is considered a collection of randomly overlapping spheres of fixed and variable diameter in three dimensions. In the spherical model, the position and diameter of grains are taken into consideration while the orientation is irrelevant. In order to generate the model of overlapping spheres, the sphere centers are distributed randomly according to the Poisson distribution. Three random Poisson-distributed numbers represent the position of center of each spherical grain in a 3D cubic lattice of arbitrary size in Cartesian coordinates. In the model of overlapping spheres of fixed diameter, the diameter of all grains is fixed to a desired value. Here as case studies, two and three spheres mutually overlap each other are considered and illustrated in Figure 1 (2D slices in the top row). It is also possible to adjust ellipses instead of spheres to generate realizations which model rocks in which grains have no more spherical shape perhaps due to inadequate displacement time before sedimentation.

One can use specific functions to distribute grains according to desired algorithms. In order to do that, position and diameter of generated grains within Cartesian coordinates obey given functions instead of random function. In the model of overlapping spheres of variable diameter, four random numbers specify the generated grains. The first three random numbers denote the center of each grain in the Cartesian coordinate system according to the Poisson-point process. To have an appropriate diameter range, a maximum and

a minimum values are chosen. The fourth random number is multiplied by the difference of the largest and the smallest grain diameters and then is summed with the smallest possible diameter to give a range of random values for grain diameter. The slices in the bottom row of Figure 1 shows the examples of 2D images of the 3D overlapping spheres of variable diameter.

To develop the prescribed model, first It is considered a particular density of sphere centers within a 3D lattice. Then the first sphere is generated, and the associated volume fraction and surface area are exactly calculated by analytical formulae. Procedure continues until the specified number of grains reaches, and then grain generation terminates. If the generated grains overlap each other, shared volume and surface area are calculated and subtracted from grain volume and surface area. The result is an artificial rock model with known exact porosity and surface area. In the next step, the Boolean model is discretized over a 3D grid of n×n×n voxels as illustrated in Figure 2.

The 3D representations of the generated Boolean models of spheres with variable diameters are shown in Figure 3.
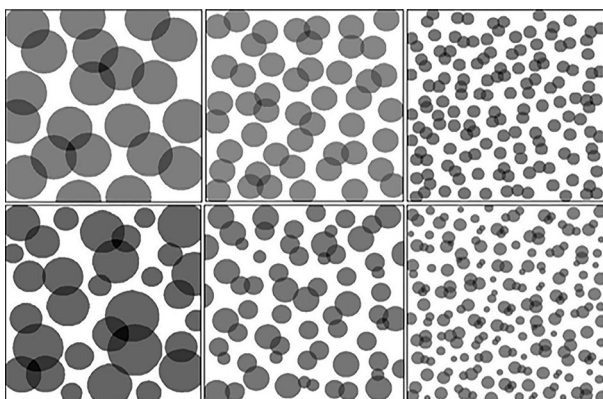


**Figure 1: Slices through the 3D Boolean model of spheres in a lattice of 10003. Top row: fixed diameter sphere model, (left) 200, (middle) 100, and (right) 50 units, Bottom row: variable diameter sphere model.**
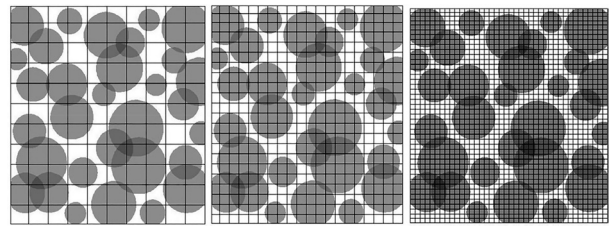


**Figure 2: Examples of 2D slices representing discretization of the Boolean model of overlapping spheres in a lattice of 10003, Mesh-Grid sizes are 100, 50, and 25 from left to right respectively.**
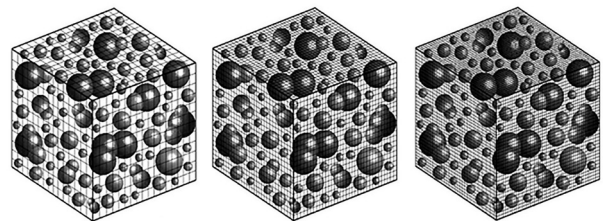


**Figure 3: 3D representations of the discretized Boolean model with the Mesh-Grid sizes of 100, 50, and 25 from left to right respectively.**

If all eight corners of a voxel fully fall into the pore space of the discretized model, this voxel contributes in pore volume calculation, while if some of the corners of a voxel place in the pore region and some of them place in the solid region, this voxel lies in pore-grain interface region and is excluded from porosity computation. The remaining voxels are counted as grain region.

Fluid saturation is one of the important physical properties which its accurate prediction is essential in various reservoir engineering calculations. The initial (static) saturation distribution as well as the dynamic saturation redistribution during production and flow Processes in petroleum reservoirs highly depends on the wetting state of the reservoir rock. In this paper, we also aim at investigating the effect of discretization on wetting and non-wetting phase saturation calculation precision. We assume that the wetting phase surrounds solid grains, and non-wetting phase

To Express Required CT-Scan Resolution for Porosity and Saturation Calculations ...

**Journal of Petroleum Science and Technology**

occupies the remaining pore space of porous media. As a consequence, the wetting and non-wetting regions are considered as two phases along with the solid grain as a third phase. One can consider two main ways to generate n-phase systems. The first method is to place particles of different phases in the lattice. The second way employs a simple geometrical overgrowth algorithm based on parallel surfaces,

Arns in 2002 [18]. In this approach, particles are covered by a parallel layer with the thickness determined by saturations desired.

The second method is adopted to generate wetting phase in the developed models. The parallel layer represents water and oil in water-wet and oil-wet rocks respectively. Thickness of the parallel layer along each curved surface and in all corners is calculated according to two phase distribution formulas that determine local phase saturation in each pore. The total integration of local saturations must be equal to overall saturation of wetting and non-wetting phases.

It should be noted that the remaining pore-phase is considered to be filled with the non-wetting phase. Since the variable-diameter grain models are more realistic, we developed saturated models for grains with variable diameters. If all eight corners of a voxel fully fall into the wetting or non-wetting phase of the discretized model, this voxel contributes in the wetting-phase or non-wetting phase saturation calculation respectively. Since the wetting phase may overlap other phases, and the corners of a voxel may place in the wetting phase, solid, or non-wetting regions. In this case, such a voxel which is in the interface is excluded from saturation calculation. The generated model is then discretized over a 3D grid of n×n×n voxels

to study the effects of mesh-grid size on wetting and non-wetting phase saturation calculations. Figure 4 shows a slice of a 3D model with artificial saturation. All the process of model development and the related calculation were coded using MATLAB R2012a.

## RESULTS AND DISCUSSION
## Effects of Discretization on Porosity Calculation

In order to prepare Boolean models, generate spheres with fixed and also variable diameters (from a Poisson distribution with λ=200) are imaginary dropped into an assumed cubic lattice of side L=1000 units to generate multiple realizations of the model.
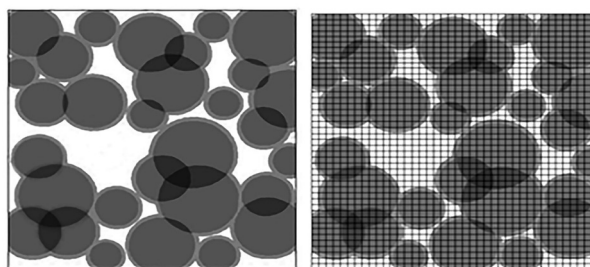


**Figure 4:** An example of a 2D slice through the 3D Boolean model of overlapping spheres with added artificial saturation in a lattice of 10003 with mesh-grid size of 25.

The chosen lattice size accompanying of spheres overlap leads to porosities lower than 20% to 30% in our work. The models are then discretized over a 3D grid of n×n×n voxels. Since the fixed number of voxels in the lattice gives results with varying accuracy for large and small grains, we consider the voxel size as a portion of the grain diameter. Hence, the number of voxels differs for each specific realization, and this leads to a more general result independent of the grain diameter. Table 1 shows the calculated porosities from

several realizations of discretized models that are compared with analytically calculated values in fixed diameter spherical models. For multiple realizations of the fixed diameter grain models, the grain diameter range from from 20 to 200 is considered with arbitrary length unit. The 3D mesh-grid (voxel) sizes range from 1 to 20 percent of the specified grain diameters as illustrated in Table 1. As a result, the number of voxels decreases as the grain diameter increases. For instance, if the voxel size is 10% of the grains with diameters of 50 and 200, the number of voxels will be 2003 and 503 respectively in a lattice of side 1000 arbitrary length unit. Note that the calculated porosity for the discretized model and the actual porosity mathematically calculated are the averages from multiple realizations. As indicated in Table 1, when the voxel size becomes smaller, values of the calculated porosities from discretized models converge to analytical values.

The results also show the similarity in relative error for all cases when the voxel size is presented as fractions of the grains diameter. For example, the relative error is about 5% when voxels are set to 5% of grains diameter. This error is about 15% and 30% for voxels which are set to 10% and 20% of the grain sizes respectively. If we consider the relative error of 5% as a satisfactory threshold for porosity calculation, the fixed diameter grain model limits us to choose voxels with size of at most 5% of grain diameter. It seems from tabulated results that when CT-scan imaging power is used to provide pixel sizes smaller than 3% of grain average diameter, negligible effects appear in calculated results. Then we generated multiple realizations of variable size models with diameters ranged from 20 to 80 units, as shown in Table 2. For each average grain diameter, we allow grains to be generated with diameters of ±10%, ±20%, and ±50% larger and smaller than the average value. For example, for average diameter of 20 units, we allow random generation of grains with 20 ±2, 20 ±4, and 20 ±10 units.

**Table 1: Porosity values of the Boolean models of fixed-diameter overlapping spheres computed on various grid sizes.**

| Voxel size as a fraction of grain diameter | Grains diameter (arbitrary length unit) | | | | | | |
|---|---|---|---|---|---|---|---|
| | 20 | 30 | 50 | 80 | 100 | 150 | 200 |
| 0.2 | 13.3 | 11.4 | 9.7 | 7.8 | 6.6 | 5.6 | 4.8 |
| 0.15 | 14.9 | 12.8 | 10.8 | 8.6 | 7.4 | 6.3 | 5.4 |
| 0.10 | 16.2 | 13.8 | 11.8 | 9.5 | 8.1 | 6.9 | 5.9 |
| 0.05 | 18.1 | 15.5 | 13.2 | 10.6 | 9.0 | 7.7 | 6.5 |
| 0.03 | 18.4 | 15.8 | 13.4 | 10.8 | 9.2 | 7.8 | 6.6 |
| 0.02 | 18.7 | 16.0 | 13.6 | 10.9 | 9.3 | 7.9 | 6.7 |
| 0.01 | 19.0 | 16.2 | 13.8 | 11.1 | 9.4 | 8.0 | 6.8 |
| Actual average porosity (%) | 19.1 | 16.3 | 13.9 | 11.2 | 9.5 | 8.1 | 6.9 |

To Express Required CT-Scan Resolution for Porosity and Saturation Calculations ...

**Journal of Petroleum Science and Technology**

**Table 2: Porosity values of the Boolean models of variable-diameter overlapping spheres computed on various grid sizes.**

| Voxel size as a fraction of grain diameter | Grains diameter (arbitrary length unit) | | | | | | | | |
|---|---|---|---|---|---|---|---|---|---|
| | 20 ±2 | 20 ±4 | 20±10 | 50 ±5 | 50 ±10 | 50 ±25 | 80 ±8 | 80 ±16 | 80 ±40 |
| 0.1 of the largest grain | 13.6 | 13.5 | 13.4 | 10.9 | 10.8 | 10.6 | 9.5 | 9.2 | 9.1 |
| 0.1 of the smallest grain | 17.5 | 17.4 | 17.1 | 14.0 | 13.9 | 13.7 | 12.1 | 11.9 | 11.7 |
| 0.05 of the largest grain | 17.9 | 17.7 | 17.5 | 14.3 | 14.1 | 14.0 | 12.4 | 12.1 | 12.0 |
| 0.05 of the smallestgrain | 18.9 | 18.7 | 18.5 | 15.1 | 14.9 | 14.7 | 13.1 | 12.8 | 12.6 |
| Actual average porosity (%) | 19.5 | 19.3 | 19.1 | 15.6 | 15.4 | 15.2 | 13.5 | 3.2 | 13.0 |

Similar to the fixed diameter model, the calculated porosity for the discretized model and the actual porosity mathematically calculated are compared together in Table 2.

In variable diameter grain models, it is essential to choose voxel sizes with attention to distributed range limits. If voxel sizes are 10% of the largest grains in each realization, about 30% relative error results in calculated porosity. But if we set voxel sizes as 10% of smallest grain, the relative error becomes only about 10%. Table 2 also shows that when voxel sizes are 5% of the largest grains, the relative error becomes 8% while if we set voxel sizes as 5% of the smallest grains, we will have only 3% error. If relative error of 5% is considered to be a satisfactory threshold, the variable diameter grain models suggest voxels with size of 8% of the smallest  grains.

## Effects of Discretization on Saturation Calculation

The variable diameter grain model is used to study the effects of discretization on wetting phase and non-wetting phase saturations.

Table 3 shows the calculated average wetting phase saturations of the models of variable-diameter spheres for the case where the grain diameters range from 16 to 25 (i.e., 20 ± 4).

**Table 3: Average wetting phase saturation values of the Boolean models of variable-diameter overlapping spheres (grain diameters: 20 ± 4) computed on various grid sizes.**

| Voxel size as a fraction of the smallest grain diameter (i.e. d = 16) | Calculated wetting phase saturation (%) | | | | | | |
|---|---|---|---|---|---|---|---|
| 0.15 | 3.0 | 6.2 | 10.6 | 14.3 | 21.5 | 28.3 | 37.0 |
| 0.10 | 3.5 | 7.1 | 12.0 | 16.2 | 24.3 | 32.4 | 41.5 |
| 0.05 | 4.2 | 8.5 | 14.3 | 19.1 | 28.5 | 38.2 | 47.8 |
| 0.03 | 4.6 | 9.4 | 14.6 | 19.5 | 29.2 | 39.0 | 48.7 |
| 0.02 | 4.8 | 9.8 | 14.8 | 19.8 | 29.7 | 39.7 | 49.3 |
| Actual wetting phase saturation (%) | 5 | 10 | 15 | 20 | 30 | 40 | 50 |

For relative error of 5% as a satisfactory threshold for saturation calculation, and for realizations in which the wetting phase saturation is larger than 15%, model offers voxels with size, at most, 5% of the diameter of the smallest grains. Conversely, for realizations in which saturation is lower than 15%, the voxel size should be 3% or less of the smallest grains diameter to have a relative error less than or equal to 5%. Authors believe this difference is caused due to this fact that for lower saturations the wetting fluid covers grain surface as form of a thin layer and hence, is more sensitive to voxel size, and relatively smaller voxels are required to distinguish wetting phase from grains and non-wetting phase. The same procedure is performed to investigate the effects of resolution and voxel sizes on non-wetting phase saturation calculations, with this difference that if all eight corners of voxels are placed in non-wetting phase, voxel is considered to count non-wetting phase saturation.

As indicated in Table 4, non-wetting phase saturation is less sensitive to voxel size, and grids with sizes, 5% of grains diameter, satisfy 95% accuracy as our chosen threshold. Authors believe that this less sensitivity, which can be explained with respect to this fact that the porous media space that occupy the non-wetting phase has less corners and sharp regions and thus do not require very small voxels for saturation calculation. Presenting required voxel sizes for calculation of wetting and non-wetting phase saturation with acceptable accuracy, in terms of average grain sizes is very valuable when we want to advance work to predict relative permeability and capillary pressure curves.
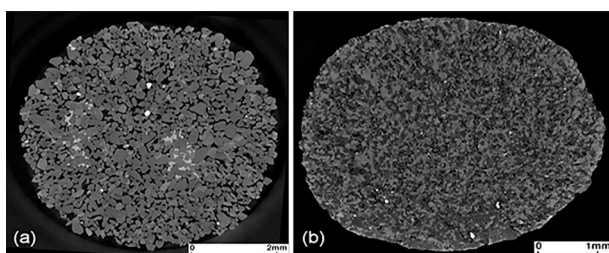
## Case Studies

Several sandstones and many other sedimentary rock types like silts, shale, and even some carbonates can be represented with variable size grain Boolean models. In order to examine the applicability of the results of this paper to real sedimentary rock samples, the micro-CT images of two core samples are used and compared with the results of the artificial models.

Figure 5 shows examples of the 2D slices through the 3D micro-CT images of sandstone (Figure 4a) and carbonate (Figure 4b) samples with voxel sizes of 2.67 and 2.44 µm respectively.

**Table 4: Average non-wetting phase saturation values of the Boolean models of variable-diameter overlapping spheres (grain diameters: 50 ± 10) computed on various grid sizes.**

| Voxel size as a fraction of the smallest grain diameter (i.e. d = 40) | Calculated non-wetting phase saturation (%) | | | | | | |
|---|---|---|---|---|---|---|---|
| 0.15 | 14.9 | 22.5 | 29.8 | 37.2 | 44.1 | 51.5 | 57.6 |
| 0.10 | 17.0 | 25.4 | 34.0 | 42.3 | 50.8 | 59.2 | 67.4 |
| 0.05 | 19.1 | 28.7 | 38.3 | 47.8 | 57.1 | 66.6 | 76.2 |
| 0.03 | 19.4 | 29.2 | 38.9 | 48.5 | 58.0 | 67.8 | 77.7 |
| 0.02 | 19.6 | 29.5 | 39.3 | 49.0 | 58.9 | 68.6 | 78.5 |
| Actual non-wetting phase saturation (%) | 20 | 30 | 40 | 50 | 60 | 70 | 80 |

To Express Required CT-Scan Resolution for Porosity and Saturation Calculations ...

**Journal of Petroleum Science and Technology**

**Figure 5: Examples of 2D slices through the 3D micro-CT tomograms of (a) sandstone and (b) carbonate core samples.**

Visual inspections of the images reveal that the sandstone sample is relatively a clean core with some clay regions near the core center. Its grains can be considered to be 0.05 to 0.3 millimeter in size. It is apparent that the sandstone sample consisted of distinct grains with approximately well-rounded shape and a variety of sizes, adequate to be represented with spherical Boolean models. The carbonate sample seems to contain three main minerals in which grains range from 0.02 to 0.1 millimeters. Despite the carbonate sample exhibits more complex grains structure, the sample may be assumed to have a potential to be compared with a Boolean model. From visual inspection of the tomograms, the voxel sizes of both images are apparently smaller than 2% of the smallest grain diameters of each core samples.

The procedure adopted in this study to examine the effect of discretization on the tomographic images is as follows. First, the original grey-scale images are exported to MATLAB. Next, we simply binarize the images and calculate the porosity based on the original resolution. Then, neighbor voxels within pore or grain regions will be merged to give upgrided voxels with side lengths of 5 % and 10 % of the smallest and largest grains. In other words, a mesh-grid is superimposed on the image in which the grid size is chosen by visual inspection of the original image and identification of the smallest and largest grains.

Moreover, It is simply taken an average voxel values to denote the values of the upgrided voxels. The new mesh-grids are used to calculate the porosity of case study samples by the same procedure as the one used for the original image. Results are presented in Table 5. In addition, a comparison graph between calculated porosities from the Boolean models of spherical grains and from the case studies is shown in Figure 6. The horizontal axis of the graph refers to the generated artificial mesh-grids as a fraction of smallest and largest grain diameters. It is evident form Figure 6 that the predicted porosities from both carbonate and sandstone case studies has a good agreement with artificial model results. Figure 6 clearly shows that the discretization errors introduced by superimposing the artificial mesh-grids over the models or actual rock images are almost the same. This is because the rock samples can be properly represented by the spherical grain models (SGMs).

**Table 5: Calculated porosities for case study samples.**

| Rock sample | Sandstone | Carbonate |
|---|---|---|
| Smallest and largest grains diameter (μm) | 50-300 | 20-100 |
| Using upgrided pixels with side length of 10% of largest grain | 12.8 | 4.6 |
| Using upgrided pixels with side length of 10% of smallest grain | 16.5 | 5.9 |
| Using upgrided pixels with side length of 5% of largest grain | 16.8 | 6.0 |
| Using upgrided pixels with side length of 5% of smallest grain | 17.8 | 6.3 |
| Actual average porosity (calculated based on the original images) | 18.3 | 6.5 |
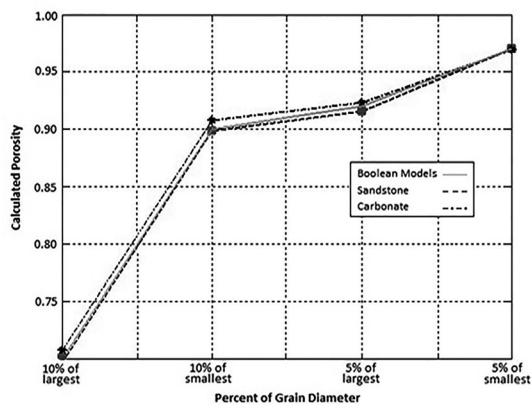
**Figure 6: A comparison of the predicted porosities from the Boolean models, carbonate and sandstone case studies.**

## CONCLUSIONS

Despite the simplicity of the Boolean model of spherical grains, it can be applicable to represent a variety of rock samples. An appropriate model of a sandstone or carbonate rock can be used to predict their properties and interrelationships. Several key findings can be summarized as follow;

(1) In simulated fixed-size grain models, the relative error for calculated porosity was about 15% when mesh-grid sizes were 10% of the grains diameter. This is while only 5% relative error was achieved when applying mesh-grids with the sizes of 5% of the grains diameter. Conversely in variable size grain models, when mesh-grids were 10% of the upper limit of grains diameter range, the relative error was about 30%. The relative error decreased to 10% when mesh-grid sizes were 10% of the lower limit grains diameter.

(2) To achieve the relative error of 5% error in porosity calculation when using the variable size grain models, one should pay a close attention to the lower limit of grain size distribution and adjust the mesh-grid size to about 8% of the smallest diameter grains.

(3) In variable size grain models, if the grain size distribution covers a wide range, it is recommended to adjust the mesh-grid size to <5% of the smallest grains.

(4) In the case of clay- or cement-rich rock samples, the relative error in porosity calculation increases since the inter granular pore-filling materials are irregular in shape and the Boolean model of spherical grains fails to properly represent the rock structure.

(5) In the case of high wetting phase saturation, i.e. larger than 15%, the mesh-grid size of 5% of the smallest grains would be sufficient to accurately calculate the wetting phase saturation using the Boolean model. Conversely, if wetting phase saturation is low (e.g., for the case of connate water saturation), mesh-grid size should be adjusted to 2 to 3% of the smallest grains diameter to decrease the relative error of saturation calculation.

(6) The calculation of non-wetting phase saturation using the Boolean model is less sensitive to the chosen mesh-grid size and mesh-grids with sizes of about 5% of the grains diameter would be sufficient. The results of this paper show that the Boolean model of spherical grains can quantitatively characterize the porosity and saturation distributions in clastic and carbonate rocks using the pre-defined mesh-grid sizes based on the rough knowledge about the grain size distribution of the rock samples. In addition, the present study can be considered as a guidance for choosing a proper voxel/ mesh-grid size in advance in image acquisition or numerical simulation of the rock samples in order to avoid gratuitously consuming computational and memory resources.

## ACKNOWLEDGEMENTS

To Express Required CT-Scan Resolution for Porosity and Saturation Calculations ...

**Journal of Petroleum
Science and Technology**

## NOMENCLATURES

| Micro-CT | : Micro-Computed Tomography |
|----------|----------------------------|
| XRT | : X–Ray Technology |
| SGMs | : Spherical Grain Models |

## REFERENCES

1. Lawrence A., Bouwer J. C., Perkins G., and Ellisman M. H., "Transform-based Backprojection for Volume Reconstruction of Large Format Electron Microscope Tilt Series," *Journal of Structural Biology*, **2006**, *154*(2), 144-167.

2. Vogel H. J., Weller U., and Schluter S., "Quantification of Soil Structure Based on Minkowski Functions," *Computers and Geosciences*, **2010**, *36*(10), 1236-1245.

3. Liu J. and Regenauer-Lieb K., "Application of Percolation Theory to Microtomography of Structured Media: Percolation Threshold, Critical Exponents, and Upscaling," *Physical Review E-Statistical, Nonlinear, and Soft Matter Physics*, **2011**, *83*(1), 016-106.

4. Adler P., "Porous Media: Geometry and Transports," (1st ed.) Stoneham MA: Butterworth-Heinemann, **1992**, 1-196.

5. Sahimi M., "Flow and Transport in Porous Media and Fractured Rock (2nd ed.)," Boschstr Germany: Wiley-VCH Verlag GmbH and Co. KGaA., **2011**, 1-217.

6. Bilodeau M., Meyer F., and Schmitt M., "Structure and Randomness: Contributions in Honor of Georges Matheron in the Fields of Geostatistics, Random Sets and Mathematical Morphology", (1st ed.) New York: Springer, **2007**, 1-354.

7. Torquato S., "Random Heterogeneous Materials: Microstructure and Macroscopic Propertie," (1st ed.) New York: Springer, **2005**, 1-237.

8. Arns C. H., Knackstedt M. A., and Mecke K. R., "Boolean Reconstructions of Complex Materials: Integral Geometric Approach," *Physical Review E*,

**2009**, *80*(5), 051-303.

9. Latief F. D. E., Irayani Z., and Fauzi U., "Resolution Dependency of Sandstone's Physical Properties," *Bruker MicroCT Meeting*, Brussels, Belgium, **2012**, 1-8.

10. Ferréol B. and Rothman D. H., "Lattice-Boltzmann Simulations of Flow through Fontainebleau Sandstone," *Transport in Porous Media*, **1995**, *20*(1), 3-20.

11. Pan C., Hilpert M., and Miller C. T., "Pore-Scale Modeling of Saturated Permeabilities in Random Sphere Packings," *Physical Review E*, 066702, **2001**.

12. Arns C. H., Knackstedt M. A., Val Pinczewski M., and Lindquist W. B., "Accurate Estimation of Transport Properties from Microtomographic Images," *Geophysical Research Letters*, **2001**, *28*(17), 3361-3364.

13. Silin D. and Patzek T., "Predicting Relative-Permeability Curves Directly From Rock Images," SPE 124974, *SPE Annual Technical Conference and Exhibition New Orleans*, Louisiana, USA, **2009**, 1-8.

14. Schneider R. and Weil W., "Stochastic and Integral Geometry," (1st ed.) Berlin Germany: Springer-Verlag, **2008**, 1-265.

15. Bilodeau M., Meyer F., and Schmitt M., "Space, Structure, and Randomnes," (1st ed.) New York: Springer, **2005**, 1-346.

16. Sobczyk K. and Kirkner D. J., "Modeling of Microstructures," (1st ed.) Cambridge: Birkhäuser Boston, **2012**, 1-238.

17. Molohanov I. S., "Estimation of the Size Distribution of Spherical Grains in the Boolean Model," *Biometrical Journal*, **1990**, *32*(7), 877-886.

18. Arns C. H., "The Influence of Morphology on Physical Properties of Reservoir Rocks," PhD Thesis, University of New South Wales, Sydney, Australia, **2002**, 1-71.